

Pairing correlation of the kagome-lattice Hubbard model with the nearest-neighbor interaction

Chen Yang(杨晨), Chao Chen(陈超), Runyu Ma(马润宇), Ying Liang(梁颖), and Tianxing Ma(马天星)

Citation: Chin. Phys. B, 2024, 33 (**10**): 107404. DOI: 10.1088/1674-1056/ad7578
Journal homepage: http://cpb.iphy.ac.cn; http://iopscience.iop.org/cpb

What follows is a list of articles you may be interested in

Half-integer Shapiro steps in MgB_2 focused He ion beam Josephson junctions

Dali Yin(殷大利), Xinwei Cai(蔡欣炜), Tiequan Xu(徐铁权), Ruining Sun(孙瑞宁), Ying Han(韩颖), Yan Zhang(张焱), Yue Wang(王越), and Zizhao Gan(甘子钊)
Chin. Phys. B, 2024, 33 (**8**): 087404. DOI: 10.1088/1674-1056/ad4d62

Two-fold symmetry of the in-plane resistance in kagome superconductor $Cs(V_{1-x}Ta_x)_3Sb_5$ with enhanced superconductivity

Zhen Zhao(赵振), Ruwen Wang(王汝文), Yuhang Zhang(张宇航), Ke Zhu(祝轲), Weiqi Yu(余维琪), Yechao Han(韩烨超), Jiali Liu(刘家利), Guojing Hu(胡国静), Hui Guo(郭辉), Xiao Lin(林晓), Xiaoli Dong(董晓莉), Hui Chen(陈辉), Haitao Yang(杨海涛), and Hong-Jun Gao(高鸿钧)
Chin. Phys. B, 2024, 33 (**7**): 077406. DOI: 10.1088/1674-1056/ad4ffa

Coevolution of superconductivity and Hall coefficient with anisotropic lattice shrinkage in compressed $KCa_2Fe_4As_4F_2$

Jinyu Han(韩金宇), Wenshan Hong(洪文山), Shu Cai(蔡树), Jinyu Zhao(赵金瑜), Jing Guo(郭静), Yazhou Zhou(周亚洲), Pengyu Wang(王鹏玉), Lixin Cao(曹立新), Huiqian Luo(罗会仟), Shiliang Li(李世亮), Qi Wu(吴奇), and Liling Sun(孙力玲)
Chin. Phys. B, 2024, 33 (**7**): 077402. DOI: 10.1088/1674-1056/ad4d65

Observation of parabolic electron bands on superconductor $LaRu_2As_2$

Xingtai Zhou(周兴泰), Geng Li(李更), Lulu Pan(潘禄禄), Zichao Chen(陈子超), Meng Li(李萌), Yanhao Shi(时延昊), Haitao Yang(杨海涛), and Hong-Jun Gao(高鸿钧)
Chin. Phys. B, 2024, 33 (**7**): 077401. DOI: 10.1088/1674-1056/ad4d63

Yi Liu(刘艺), Jing Li(厉静), Wu-Zhang Yang(杨武璋), Jia-Yi Lu(卢佳依), Bo-Ya Cao(曹博雅), Hua-Xun Li(李华旬), Wan-Li Chai(柴万力), Si-Qi Wu(武思祺), Bai-Zhuo Li(李佰卓), Yun-Lei Sun(孙云蕾), Wen-He Jiao(焦文鹤), Cao Wang(王操), Xiao-Feng Xu(许晓峰), Zhi Ren(任之), and Guang-Han Cao(曹光旱)
Chin. Phys. B, 2024, 33 (**5**): 057401. DOI: 10.1088/1674-1056/ad1c5e

Co-doped $BaFe_2As_2$ Josephson junction fabricated with a focused helium ion beam

Ziwen Chen(陈紫雯), Yan Zhang(张焱), Ping Ma(马平), Zhongtang Xu(徐中堂), Yulong Li(李宇龙), Yue Wang(王越), Jianming Lu(路建明), Yanwei Ma(马衍伟), and Zizhao Gan(甘子钊)
Chin. Phys. B, 2024, 33 (**4**): 047405. DOI: 10.1088/1674-1056/ad21f7

SPECIAL TOPIC — Recent progress on kagome metals and superconductors

Pairing correlation of the kagome-lattice Hubbard model with the nearest-neighbor interaction

Chen Yang(杨晨)[1], Chao Chen(陈超)[2,1], Runyu Ma(马润宇)[1], Ying Liang(梁颖)[1], and Tianxing Ma(马天星)[1,3,†]

[1] *School of Physics and Astronomy, Beijing Normal University, Beijing* 100875, *China*
[2] *Department of Basic Courses, Naval University of Engineering, Wuhan* 430033, *China*
[3] *Key Laboratory of Multiscale Spin Physics (Ministry of Education), Beijing Normal University, Beijing* 100875, *China*

(Received 15 June 2024; revised manuscript received 23 August 2024; accepted manuscript online 30 August 2024)

A recently discovered family of kagome lattice materials, AV_3Sb_5 ($A = \mathrm{K}, \mathrm{Rb}, \mathrm{Cs}$), has attracted great interest, especially in the debate over their dominant superconducting pairing symmetry. To explore this issue, we study the superconducting pairing behavior within the kagome-lattice Hubbard model through the constrained path Monte Carlo method. It is found that doping around the Dirac point generates a dominant next-nearest-neighbor-d pairing symmetry driven by on-site Coulomb interaction U. However, when considering the nearest-neighbor interaction V, it may induce nearest-neighbor-p pairing to become the preferred pairing symmetry. Our results provide useful information to identify the dominant superconducting pairing symmetry in the AV_3Sb_5 family.

Keywords: kagome-lattice Hubbard model, superconductivity, pairing symmetry, CPMC

PACS: 74.20.Rp, 74.72.Gh, 71.10.Fd, 02.70.Ss **DOI:** 10.1088/1674-1056/ad7578

1. Introduction

The discovery of the superconducting AV_3Sb_5 family has attracted tremendous attention due to their exotic properties.[1–6] These materials offer an important platform to explore a variety of novel quantum phases of electron correlations[7–12] and their physical properties are closely related to their unique electronic structure. Specifically, the crystal structure of AV_3Sb_5 forms a layered kagome system. Accompanying the strong frustration in the kagome lattice, its electronic structure has flat bands and Dirac cones, which give rise to a number of intriguing properties, including quantum anomalous Hall effect,[13–15] charge density wave order,[16,17] Z_2 topological invariant,[9,18] and superconductivity.[19,20] Among them, the possible dominant superconducting pairing symmetry is highly debated. Thermal conductivity measurements and a V-shaped pairing gap suggest an unconventional nodal superconductivity in AV_3Sb_5.[21–24] On the other hand, measurements of magnetic penetration depth and the effects of magnetic impurities suggest the absence of sign-change in the superconducting order parameter,[25–27] pointing to a nodeless s-wave superconductivity. Therefore, reconciling the contradictions in experimental evidence is a significant challenge to overcome.

To study the superconductivity in AV_3Sb_5 family, a Hubbard-type model defined on a kagome lattice has been studied intensively.[28–33] For example, s-wave superconductivity, driven by on-site Coulomb interactions, has been proposed in the kagome-lattice Hubbard model by using the determinant quantum Monte Carlo method.[34] In correlated electron systems, the van Hove singularities (VHSs) in the density of states may play an essential role in novel superconducting phenomena.[35] In a kagome lattice, calculations around upper van Hove filling by random-phase-approximation indicate that d-wave or f-wave pairing symmetries are likely more favorable.[36,37] Additional research through an analytic renormalization group analysis has suggested $\mathrm{d}+\mathrm{id}$ superconductivity in the kagome-lattice Hubbard model around the van Hove filling, with enhancements attributed to long-range Coulomb interactions, which reduce sublattice interference effects.[38–40] Furthermore, it has been theoretically proposed that this chiral $\mathrm{d}+\mathrm{id}$ superconductivity can even become the dominant order in the $1/6$ hole-doped kagome lattice by using the variational cluster approach.[14] These theoretical discoveries intertwined with experimental results have deepened our understanding of pairing states and mechanisms. However, different methods lead to different results and conflicting experimental evidence has caused ongoing controversy. Due to the extensive experimental controversy and theoretical proposal regarding the superconducting pairing and its mechanism in AV_3Sb_5 compounds, identify the pairing symmetry of the superconducting order parameter by some exact numerical method is urgently required.[38,41–45]

In this paper, we employ the constrained path Monte Carlo (CPMC) method to study the pairing correlation in the kagome-lattice Hubbard model. Simulations are mainly performed on 3×6^2 lattices with periodic boundary conditions. We present our unbiased numerical results of ground-state pairing correlation functions for different pairing sym-

†Corresponding author. E-mail: txma@bnu.edu.cn

© 2024 Chinese Physical Society and IOP Publishing Ltd

metries. Our results show that the on-site Coulomb interaction U causes the next-nearest neighbor (NNN) d-wave (NNN-d) pairing to dominate over other pairing symmetries. However, as we introduce the nearest-neighbor (NN) interaction with $V = -1.0$, the system favors the NN p-wave (NN-p) pairing. The rest of this paper is organized as follows. Section 2 presents the model we are going to investigate, along with the computational methodology employed. In Section 3, the pairing correlations are discussed. A summary is given in Section 4.

2. Theoretical method

The kagome-lattice Hubbard model is described by the Hamiltonian

$$H = -t \sum_{\langle i,j\rangle\sigma} c^{\dagger}_{i\sigma} c_{j\sigma} + U \sum_{i} n_{i\uparrow} n_{i\downarrow} + V \sum_{\langle i,j\rangle\sigma} n_{i\sigma} n_{j\sigma}. \quad (1)$$

Here, $c^{\dagger}_{i\sigma}$ ($c_{i\sigma}$) creates (annihilates) electrons at site i in the kagome lattice with spin σ ($\sigma = \uparrow, \downarrow$). t represents the NN hopping integral. $n_{i\sigma} = c^{\dagger}_{i\sigma} c_{i\sigma}$ denotes the electron number of spin σ at site i. $\langle i, j\rangle$ denotes the NNs. U is the on-site Hubbard interaction, while the interaction between NN sites is denoted by V. In our computational process, we set the hopping amplitude $t = 1$.

As observed, each site is surrounded by four NN sites, four NNN sites, and six third-NN (3rd NN) sites in the kagome lattice. Figure 1(a) shows the structure of the kagome lattice. Figure 1(b) displays the Brillouin zone of the kagome lattice, where K, M, and Γ represent the high-symmetry points. As seen in Fig. 1(c), the kagome lattice features three bands, including two cone-shaped Dirac bands and one distinctive flat band. At K point, there is a Dirac point. While at M point, there are two van Hove singularities.

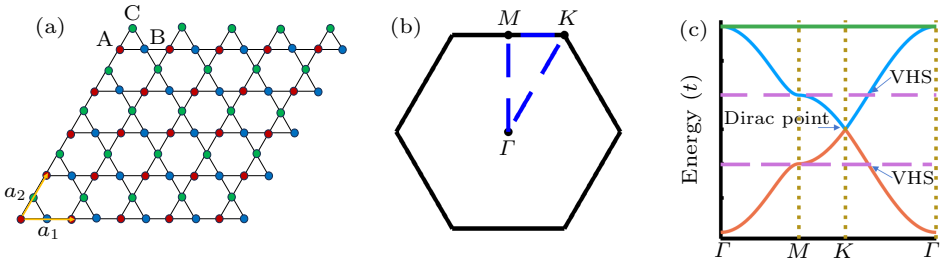


Fig. 1. (a) The structure of the kagome lattice with lattice vectors a_1 and a_2. In each unit cell, the sublattice is labeled as A (red dots), B (blue dots), and C (green dots). (b) The Brillouin zone of the kagome lattice. (c) The band structure of the tight-binding kagome model.

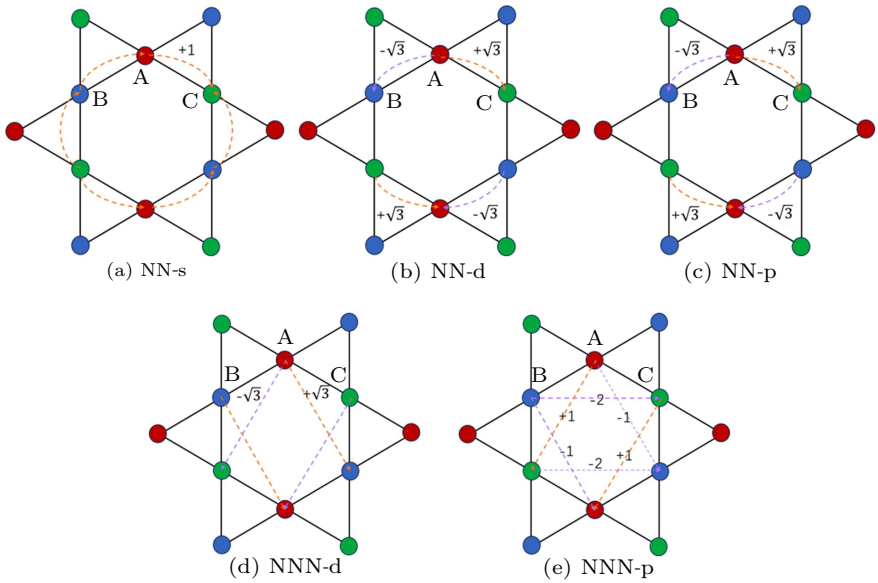


Fig. 2. Pairing symmetries between the sites in the kagome lattice: (a) NN-s, (b) NN-d, (c) NN-p, (d) NNN-d, and (e) NNN-p. The orange and purple arrows represent positive and negative pairings, respectively.

To study the superconducting pairing behavior, we define the pairing correlation function as follows:

$$C_{\alpha}(r) = \frac{1}{N_{\mathrm{cor}}(r)} \times \sum_{ij} \delta\left(\left|R_i - R_j\right| - r\right) \left\langle \Delta^{\dagger}_{\alpha}(i) \Delta_{\alpha}(j) \right\rangle, \quad (2)$$

where $N_{\mathrm{cor}}(r) = \sum_{ij} \delta\left(\left|R_i - R_j\right| - r\right)$ stands for the number of correlations whose length is r, and α represents different pairing symmetry. The corresponding order parameter for spin-triplet and spin-singlet pairings $\Delta^{\dagger}_{\alpha}(i)$ is defined as

$$\Delta^{\dagger}_{\alpha}(i) = \sum_{l} f^{\dagger}_{\alpha}(\delta_l) \left(c_{i\uparrow} c_{i+\delta_l\downarrow} \pm c_{i\downarrow} c_{i+\delta_l\uparrow}\right)^{\dagger}. \quad (3)$$

Here, $f_\alpha(\delta_l)$ is the form factor of pairing function and the vectors δ_l denote the connections between sites. We reference five kinds of pairing forms from the kagome lattice,[36] which are plotted in Fig. 2. The pairing function in momentum space is converted into real-space pairing using the Fourier transform and lattice harmonics. This figure displays the real-space pairing symmetries between the sites.

To identify the dominant pairing symmetry in the investigated system, we utilize the CPMC method to study the long-range part of the pairing correlation function in the kagome-lattice Hubbard model, which can effectively extract ground state properties while avoiding the sign problem.[33,36,46–49] It extracts the ground state from an initial guess by exploring different paths in the Slater determinant space.[33] To address potential sign issues, we employ a constrained-path approximation in the CPMC algorithm.[36,48] In the CPMC method, extensive benchmark calculations showed that the systematic error induced by the constraint is within a few percent and the ground-state observables are insensitive to the choice of trial wave function. In our CPMC simulations, we employ closed-shell electron fillings and use the corresponding free-electron $U = 0$ wave function as the trial wave function.[50–52] In a typical run, we set the average number of random walkers to be 1200 and the time step $\Delta\tau = 0.05$. We perform measurements in 40 blocks of 320 Monte Carlo steps to ensure statistical independence.

3. Results and discussion

We first examine the dominant pairing symmetry for a fixed $U = 3.0$ at different electron fillings. In Fig. 3, we present the long-range part of the pairing correlations C_α with different symmetries as a function of distance r on the 3×6^2 lattices at the electron filling $\langle n \rangle \approx 0.704$ and $\langle n \rangle \approx 0.630$ corresponding to closed-shell around the Dirac point $\langle n \rangle \approx 0.667$. In Fig. 3(a), the electron filling is set to $\langle n \rangle \approx 0.704$, and in Fig. 3(b) is set to $\langle n \rangle \approx 0.630$. Both Figs. 3(a) and 3(b) display that the NNN-d pairing symmetry plays a dominant role with on-site interaction $U = 3.0$. As can be seen in Fig. 3(a), the NN-s oscillates around zero at long-range distances, indicating that the NN-s pairing correlation between the NN electrons is very weak or nearly absent. Our findings suggest that doping around the Dirac point generates a dominant NNN-d pairing symmetry driven by on-site Coulomb interaction U. In our present work, we are mainly concerned with the pairing correlation function versus distance for different pairing symmetries. For all long-range distances between electron pairs, the competition between d-wave and p-wave correlation plays a crucial role in the selection of the dominant pairing symmetry. By thoroughly considering the effects of both NN and NNN pairings, we demonstrate that the NNN-d pairing symmetry dominates, which provides a guideline for understanding the superconducting pairing symmetries in the kagome-lattice Hubbard model.

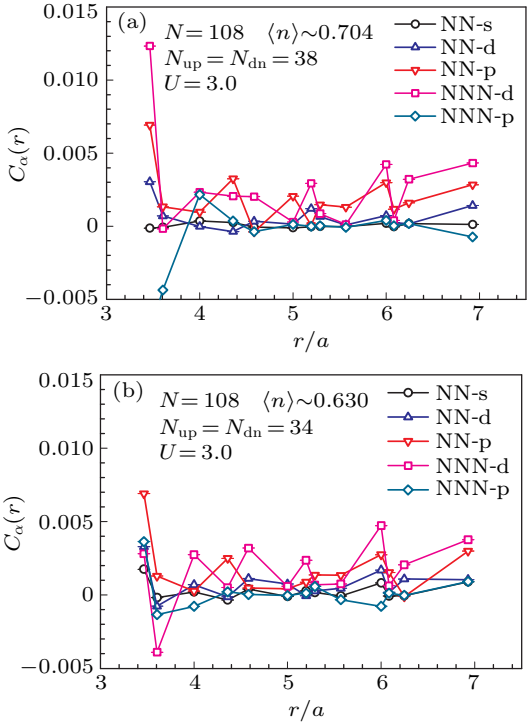


Fig. 3. Pairing correlations C_α as a function of distance r for different pairing symmetries with $U = 3.0$ at (a) $\langle n \rangle \approx 0.704$ and (b) $\langle n \rangle \approx 0.630$ and $L = 6$.

To further explore the long-range part of the dominant NNN-d pairing correlation function versus distance, we set varying electron filling values to $\langle n \rangle \approx 0.630$, 0.704, and 0.981. In Fig. 4, we present $C_\alpha(r)$ as a function of distance r for different electron fillings, with NNN-d pairing correlations shown at $U = 3.0$. Figure 4 demonstrates that the superconducting pairing with NNN-d symmetry is the weakest with hole doping at $\langle n \rangle \approx 0.981$, which indicates that the NNN-d pairing symmetry is suppressed when the system is doped in proximity to half-filling. The NNN-d pairing correlation begins to drop quickly from $r \approx 3.4$ and reaches its minimum value at $r \approx 3.6$ for different electron fillings. Additionally, we observe that the value of NNN-d pairing correlation function is consistently positive at $\langle n \rangle \approx 0.704$.

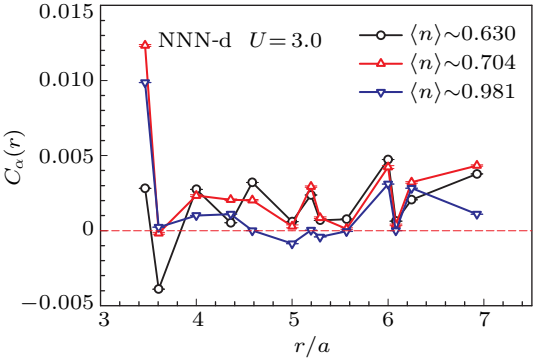


Fig. 4. Long-range part of NNN-d pairing correlations with different electron fillings at $\langle n \rangle \approx 0.630$, $\langle n \rangle \approx 0.704$, and $\langle n \rangle \approx 0.981$ at $U = 3.0$.

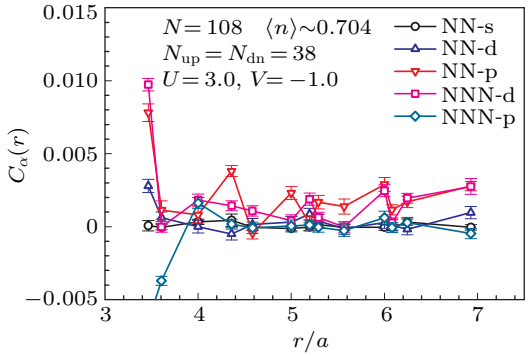


Fig. 5. Pairing correlations $C_\alpha(r)$ as a function of distance r for different pairing symmetries with $U=3.0$ and $V=-1.0$.

To study the effect of the NN interaction V on pairing symmetries, we calculate the $C_\alpha(r)$ for different pairing symmetries at $\langle n\rangle\approx0.704$, $U=3.0$ and $V=-1.0$ in Fig. 5. As the data illustrates, applying V enhances the NN-p pairing. This indicates that the NN interaction V causes the NN-p to surpass the NNN-d and take the lead in pairing symmetry. Based on the above analysis, we speculate that the negative V affects the NN-p symmetry and the NNN-d symmetry differently, leading to a shift in the dominant pairing symmetry.

As illustrated in Fig. 6(a), comparing the results for the NN interaction $V=-1.0$, 0.0, and 1.0, it is evident that the strength of the NN-p pairing symmetry is enhanced with decreasing V. Further observing Fig. 6(b), we find that when $V=0.0$, the NNN-d pairing correlation function is the largest. Figure 6(c) presents the long-range parts of various pairing correlations as a function of V, in which we sum up the correlations whose distance is three times larger than lattice constant a, and we denote it by $D_\alpha(r/a>3)$. It can be concluded that a negative V enhances the NN-p pairing, while both positive and negative V suppress the NNN-d pairing. This elucidates why, at $V=-1.0$, the NN-p symmetry supersedes the NNN-d symmetry, emerging as the dominant one.

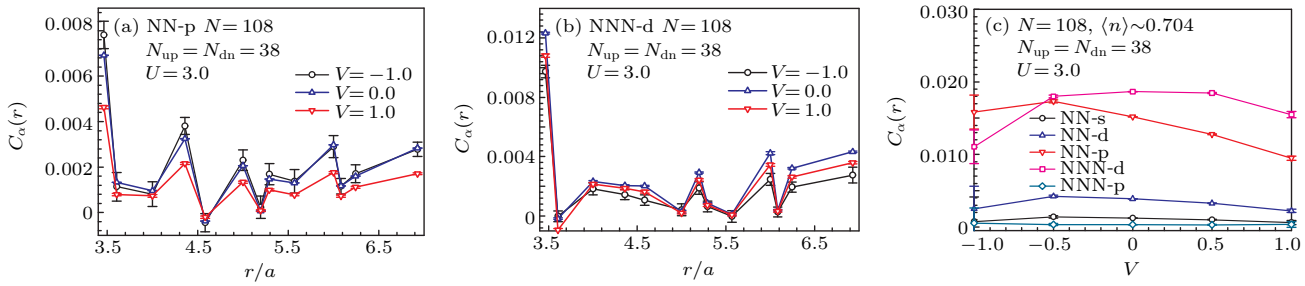


Fig. 6. Pairing correlations $C_\alpha(r)$ as a function of distance r for (a) NN-p (b) NNN-d with different V at $U=3.0$. (c) Pairing correlations $D_\alpha(r/a>3)$ as a function of the NN interaction V at $U=3.0$ on the $L=6$ lattice for different pairing symmetries.

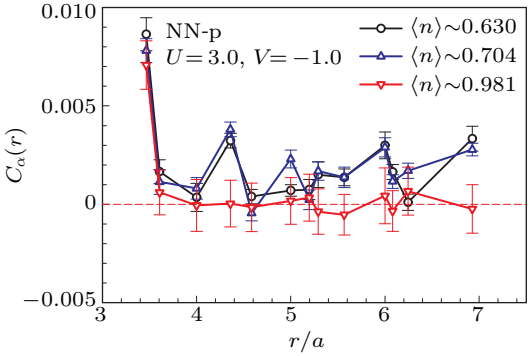


Fig. 7. Long-range part of NN-p pairing correlations with different electron fillings at $\langle n\rangle\approx0.630$, $\langle n\rangle\approx0.704$, and $\langle n\rangle\approx0.981$ at $U=3.0$ and $V=-1.0$.

Figure 4 displays the long-range part of NNN-d pairing correlations with different electron fillings at $U=3.0$ and $V=0.0$. Applying $V=-1.0$ makes the NN-p pairing symmetry dominate. Therefore, we focus on the analysis of the pairing correlations of NN-p symmetry at different electron fillings with $U=3.0$ and $V=-1.0$. Figure 7 illustrates that the NN-p pairing correlation is the weakest with hole doping close to half-filling but reaches its maximum at $\langle n\rangle\approx0.704$. The trends in the variation of $C_\alpha(r)$ at $\langle n\rangle\approx0.630$ and $\langle n\rangle\approx0.704$ show a considerable degree of similarity. Furthermore, at $\langle n\rangle\approx0.981$, the NN-p pairing correlation oscillates around zero for distances r greater than approximately 3.5.

Finally, we study the effects of system size on pairing. Our simulations are performed on a larger lattice of $L=9$ at $U=3.0$ and $\langle n\rangle\approx0.683$, with a closed-shell filling of $N_{\rm up}=N_{\rm dn}=83$. The results are shown in Fig. 8, with the impact of on-site repulsive interaction U, the NNN-d pairing symmetry dominates is consistent with our previous results. This further confirms that the finite-size effect does not affect the dominant pairing symmetry.

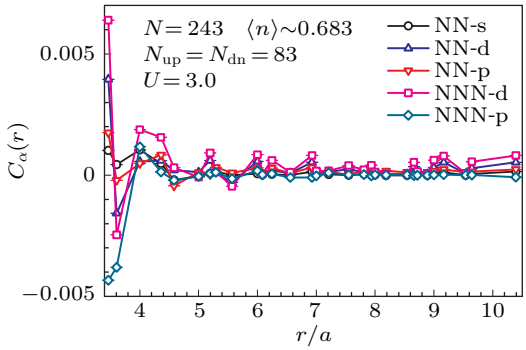


Fig. 8. Pairing correlations $C_\alpha(r)$ as a function of distance r for different pairing symmetries with $U=3.0$ at $N_{\rm up}=N_{\rm dn}=83$ and $L=9$.

4. Conclusion

In summary, we have studied the superconducting pairing correlation of the kagome-lattice Hubbard model using the CPMC method. In calculating the pairing correlation functions, we were mainly concerned with the closed-shell case. Our numerical results show that in the presence of on-site Coulomb interaction U, the NNN-d pairing symmetry plays a dominant role. Upon introducing the NN interaction V, NN-p pairing may surpass NNN-d pairing and become the dominant pairing symmetry. Moreover, our result indicates a very weak lattice-size effect. When considering the NN interaction V, our findings suggest a novel competition between NN-p and NNN-d pairing correlations. In all, our results provide a deeper understanding of superconducting pairing mechanisms in the kagome lattice model.

Acknowledgements

Project supported by Beijing Natural Science Foundation (Grant No. 1242022). The numerical simulations in this work were performed at HSCC of Beijing Normal University.

References

[1] Yu F H, Ma D H, Zhuo W Z, Liu S Q, Wen X K, Lei B, Ying J J and Chen X H 2021 *Nat. Commun.* **12** 3645
[2] Liang Z, Hou X, Zhang F, Ma W, Wu P, Zhang Z, Yu F, Ying J J, Jiang K, Shan L, Wang Z and Chen X H 2022 *Sci. Adv.* **8** eabl4108
[3] Xu L and Yang F 2024 *Chin. Phys. B* **33** 027101
[4] Li Y, Xi W, Dong Z, Yao Z, Yu S and Li J 2024 *Chin. Phys. B* **33** 017404
[5] Wang Y, Liu Y and Hao Z, *et al*. 2023 *Chin. Phys. Lett.* **40** 037102
[6] Jiang Y, Yu Z, Wang Y, Lu T, Meng S, Jiang K and Liu M 2022 *Chin. Phys. Lett.* **39** 047402
[7] Ortiz B R, Teicher S M L, Hu Y, Zuo J L, Sarte P M, Schueller E C, Milinda Abeykoon A M, Krogstad M J, Rosenkranz S, Osborn R, Seshadri R, Balents L, He J and Wilson S D 2020 *Phy. Rev. Lett.* **125** 247002
[8] Mine A, Zhong Y, Liu J, Suzuki T, Najafzadeh S, Uchiyama T, Yin J X, Wu X, Shi X, Wang Z, Yao Y and Okazaki K 2024 arXiv:2404.18472v1 [cond-mat.supr-con]
[9] Tan H, Liu Y, Wang Z and Yan B 2021 *Phys. Rev. Lett.* **127** 046401
[10] Mielke III C, Das D, Yin J X, Liu H, Gupta R, Jiang Y X, Medarde M, Wu X, Lei H C, Chang J J, Dai P, Si Q, Miao H, Thomale R, Neupert T, Shi Y, Khasanov R, Hasan M Z, Luetkens H and Guguchia Z 2022 *Nature* **602** 245
[11] Nie L, Sun K, Ma W, Song D, Zheng L, Liang Z, Wu P, Yu F, Li J, Shan M, Zhao D, Li S, Kang B, Wu Z, Zhou Y, Liu K, Xiang Z, Ying J, Wang Z, Wu T and Chen X 2022 *Nature* **604** 59
[12] Ding P, Lee C H, Wu X and Thomale R 2022 *Phys. Rev. B* **105** 174518
[13] Ptok A, Kobiałka A, Sternik M, Łażewski J, Jochym P T, Oleś A M and Piekarz P 2022 *Phys. Rev. B* **105** 235134
[14] Yu S L and Li J X 2012 *Phys. Rev. B* **85** 144402
[15] Mi X R, Yang K Y, Gan Y H, Zhang L, Wang A F, Chai Y S, Zhou X Y and He M Q 2023 *Tungsten* **5** 300
[16] Xu Y, Ni Z, Liu Y, Ortiz B R, Deng Q, Wilson S D, Yan B, Balents L and Wu L 2022 *Nat. Phys.* **18** 1470
[17] Li H, Oh D, Kang M, Zhao H, Ortiz B R, Oey Y, Fang S, Ren Z, Jozwiak C, Bostwick A, Rotenberg E, Checkelsky J G, Wang Z, Wilson S D, Comin R and Zeljkovic I 2023 *Phys. Rev. X* **13** 031030
[18] Liang Z, Hou X, Zhang F, Ma W, Wu P, Zhang Z, Yu F, Ying J J, Jiang K, Shan L, Wang Z and Chen X H 2021 *Phys. Rev. X* **11** 031026
[19] Yin J X, Zhang S S, Chang G, Wang Q, Tsirkin S S, Guguchia Z, Lian B, Zhou H, Jiang K, Belopolski I, Shumiya N, Multer D, Litskevich M, Cochran T A, Lin H, Wang Z, Neupert T, Jia S, Lei H and Hasan M Z 2019 *Nat. Phys.* **15** 443
[20] Profe J B, Klebl L, Grandi F, Hohmann H, Dürrnagel M, Tschwemmer T, Thomale R and Kennes D M 2024 arXiv:2402.11916v1 [cond-mat.str-el]
[21] Zhao C C, Wang L S, Xia W, Yin Q W, Ni J M, Huang Y Y, Tu C P, Tao Z C, Tu Z J, Gong C S, Lei H C, Guo Y F, Yang X F and Li S Y 2021 arXiv:2102.08356 [cond-mat.supr-con]
[22] Kang M, Fang S, Kim J K, Ortiz B R, Ryu S H, Kim J, Yoo J, Sangiovanni G, Sante D D, Park B G, Jozwiak C, Bostwick A, Rotenberg E, Kaxiras E, Wilson S D, Park J H and Comin R 2022 *Nat. Phys.* **18** 301-308
[23] Feng X, Jiang K, Wang Z and Hu J 2021 *Science Bulletin* **66** 1384
[24] Denner M M, Thomale R and Neupert T 2021 *Phys. Rev. Lett.* **127** 217601
[25] Xu H S, Yan Y J, Yin R, Xia W, Fang S, Chen Z, Li Y, Yang W, Guo Y and Feng D L 2021 *Phys. Rev. Lett.* **127** 187004
[26] Duan W, Nie Z, Luo S, Yu F, Ortiz B R, Yin L, Su H, Du F, Wang A, Chen Y, Lu X, Ying J, Wilson S D, Chen X, Song Y and Yuan H 2021 *Sci. China Phys. Mech. Astron.* **64** 107462
[27] Wulferding D, Lee S, Choi Y, Yin Q, Tu Z, Gong C, Lei H, Yousuf S, Song J, Lee H, Park T and Choi K Y 2022 *Phys. Rev. Research* **4** 023215
[28] Kaufmann J, Steiner K, Scalettar R T, Held K and Janson O 2021 *Phys. Rev. B* **104** 165127
[29] Bulut N, Koshibae W and Maekawa S 2005 *Phys. Rev. Lett.* **95** 037001
[30] Gu Y, Zhang Y, Feng X, Jiang K and Hu J 2022 *Phys. Rev. B* **105** L100502
[31] Wen C, Zhu X, Hao N, Guo H and Feng S 2022 *Phys. Rev. B* **105** 245131
[32] Wang Z, Jiang Y X, Yin J X, Li Y, Wang G Y, Huang H L, Shao S, Liu J, Zhu P, Shumiya N, Hossain M S, Liu H, Shi Y, Dua Jn, Li X, Chang G, Dai P, Ye Z, Xu G, Wang Y, Zheng H, Jia J, Hasan M Z and Yao Y 2021 *Phys. Rev. B* **104** 075148
[33] Shi H, Jiménez-Hoyos C A, Rodríguez-Guzmán R, Scuseria G E and Zhan S 2014 *Phys. Rev. B* **89** 125129
[34] Zhu X, Han W, Feng S and Guo H 2023 *Phys. Rev. Res.* **5** 023037
[35] Ma T, Yang F, Yao H and Lin H Q 2014 *Phys. Rev. B* **90** 245114
[36] Wu X, Schwemmer T, Müller T, Consiglio A, Sangiovanni G, Sante D D, Iqbal Y, Hanke W, Schnyder A P, Denner M M, Fischer M H, Neupert T and Thomale R 2021 *Phys. Rev. Lett.* **127** 177001
[37] Kiesel M L, Platt C and Thomale R 2013 *Phys. Rev. Lett.* **110** 126405
[38] Kiesel M L and Thomale R 2012 *Phys. Rev. B* **86** 121105
[39] Wang W S, Li Z Z, Xiang Y Y and Wang Q H 2013 *Phys. Rev. B* **87** 115135
[40] Yang Q G, Yao M, Wang D and Wang Q H 2024 *Phys. Rev. B* **109** 075130
[41] Liu J and Zhou T 2024 *Phys. Rev. B* **109** 054504
[42] Wilson S D and Ortiz B R 2023 arXiv:0809.0872v1 [cond-mat.supr-con]
[43] Jiang K, Wu T, Yin J X, Wang Z, Hasan M Z, Wilson S D, Chen X and Hu J 2023 *National Science Review* **10** nwac199
[44] Rømer A T, Bhattacharyya S, Valentí R, Christensen M H and Andersen B M 2022 *Phys. Rev. B* **106** 174514
[45] Neupert T, Denner M M, Yin J X, Thomale R and Hasan M Z 2022 *Nat. Phys.* **18** 137
[46] Zhang S, Carlson J and Gubernatis J E 1997 *Phys. Rev. Lett.* **78** 4486
[47] Zhang S, Carlson J and Gubernatis J E 1997 *Phys. Rev. B* **55** 7464
[48] Liu G, Fang S, Zheng X, Huang Z and Lin H 2018 *J. Phys.: Condens. Matter* **30** 445604
[49] Fang S C, Zheng X J, Lin H Q and Huang Z B 2021 *J. Phys.: Condens. Matter* **33** 025601
[50] Wang J, Zhang X, Ma R, Yang G, Castro E V and Ma T 2022 *Phys. Rev. B* **106** 134513
[51] Dai H, Ma R, Zhang X, Guo T and Ma T 2023 *Phys. Rev. B* **107** 245106
[52] Ma T, Huang Z, Hu F and Lin H Q 2011 *Phys. Rev. B* **84** 121410(R)